Cancellation of Aerosol Indirect Effects in Marine Stratocumulus through Cloud Thinning

ROBERT WOOD

University of Washington, Seattle, Washington

(Manuscript received 5 June 2006, in final form 18 September 2006)

ABSTRACT

Applying perturbation theory within a mixed layer framework, the response of the marine boundary layer (MBL) cloud thickness h to imposed increases of the cloud droplet concentration N_d as a surrogate for increases in cloud condensation nuclei (CCN) concentrations is examined. An analytical formulation is used to quantify the response and demonstrate theoretically that for the range of environmental conditions found over the subtropical eastern oceans, on time scales of less than a day, the cloud thickness feedback response is largely determined by a balance between the moistening/cooling of the MBL resulting from the suppression of surface precipitation, and the drying/warming resulting from enhanced entrainment resulting from increased turbulent kinetic energy. Quantifying the transient cloud response as a ratio of the second to the first indirect effects demonstrates that the nature of the feedback is critically dependent upon the nature of the unperturbed state, with the cloud-base height z_{cb} being the single most important determinant. For $z_{cb} < 400$ m, increasing N_d leads to cloud thickening in accordance with the Albrecht hypothesis. However, for $z_{cb} > 400$ m, cloud thinning occurs, which results in a feedback effect that increasingly cancels the Twomey effect as z_{cb} increases. The environmental conditions favoring an elevated cloud base are relatively weak lower-tropospheric stability and a dry free troposphere, although the former is probably more important over the subtropical eastern oceans. On longer time scales an invariable thickening response is found, and thus accurate quantification of the aerosol indirect effects will require a good understanding of the processes that control the time scale over which aerosol perturbations are modified.

1. Introduction

Marine boundary layer (MBL) clouds cover a third of the world's oceans and have a profound impact upon its radiative balance (Klein and Hartmann 1993). Extensive sheets of stratocumulus swath the eastern subtropical ocean regions and influence their climate (Ma et al. 1996). It is therefore of great importance to understand the processes that control the radiative properties of these clouds. Climate models (e.g., Haywood and Boucher 2000) support the idea originally proposed by Twomey (1977) that increasing the concentration of cloud condensation nuclei (CCN) by anthropogenic means may increase the albedo of clouds. However, there is poor consensus as to the magnitude of the increase (Lohmann and Feichter 2005). Forward models (physical climate prediction models) generally show a much stronger total anthropogenic aerosol signature than is implied by inverse calculations (Anderson et al. 2003). The reasons for the discrepancy are unclear, but may be rooted in the difficulties in understanding processes that control the CCN population in the MBL (Bates et al. 1998; Katoshevski et al. 1999), and also from an incomplete knowledge of cloud feedbacks (Lohmann and Feichter 2005).

A key hypothesized feedback is the increase in cloud lifetime, thickness, and/or coverage (Albrecht 1989) resulting from precipitation suppression in clouds forming when CCN concentrations are elevated. Most global climate models with a treatment of the so-called *indirect effects,* that is, the effects of aerosols on cloud albedo, show that increased CCN concentration results in increased cloud droplet concentration N_d (Ghan et al. 2001). The smaller, more numerous cloud droplets coalesce less efficiently, which suppresses precipitation. In the models, this reduced cloud water sink contributes to feedback effects that are of the same sign and as strong as the Twomey effect Lohmann and Feichter (2005). However, large-eddy simulations (Ackerman 2004) of MBL clouds, with a range of microphysical and

Corresponding author address: Dr. Robert Wood, Atmospheric Sciences, University of Washington, Seattle, WA 98195.
E-mail: robwood@atmos.washington.edu

DOI: 10.1175/JAS3942.1

environmental forcings, cast some doubt on the ability of climate models to accurately simulate these effects.

In general, the reduced cloud water sink acts to moisten and cool the MBL, lowering the cloud base. If this was the only response then increasing N_d would always lead to thicker clouds as hypothesized by Albrecht (1989), thus adding to increases in cloud reflectance from the reduced droplet size (Twomey 1977). However, the decrease in precipitation also reduces its stabilizing effect, leading to stronger turbulence in the MBL and increasing the rate at which warm, dry overlying air is entrained (Pincus and Baker 1994; Stevens et al. 1998). This drying and warming effect opposes the moistening/cooling resulting from changes in surface precipitation and can, under certain circumstances, completely cancel it, resulting in clouds that become thinner as N_d is increased (Jiang et al. 2002; Ackerman 2004). It is crucial therefore to understand the factors controlling this feedback response.

Here, we examine the response of the cloud thickness to perturbations of N_d using a mixed layer framework. We first derive an analytical approximation that casts light onto the processes controlling the cloud thickness response, and then proceed to demonstrate its utility using numerical solutions of the mixed layer model. The analytic formulation is then used to understand why the cloud-base height is a critical parameter that determines the sign and magnitude of the cloud thickness feedback on time scales of less than a day. The implications of the results for the ability of climate models to simulate the key physical processes necessary to accurately predict feedback response are discussed.

2. Analytical formulation

We use a mixed layer model (MLM), a simple but useful thermodynamic model of the cloud-capped MBL (Lilly 1968; Caldwell et al. 2005). In the MLM, cloud thickness $h = z_i - z_{\rm cb}$, where z_i is the height of the base of the cloud-top inversion and $z_{\rm cb}$ is the cloud-base height. Given fixed external forcings [sea surface temperature (SST), lower-tropospheric divergence D, and the temperature and moisture of the overlying air], the MLM determines the steady-state (equilibrium) temperature, humidity, and depth of the MBL, and therefore $z_{\rm cb}^{(e)}$ and $z_i^{(e)}$, where the superscript $^{(e)}$ is used to denote an equilibrium value. We examine the effects of a step change in N_d upon h by considering the perturbation induced in the equilibrium state.

The response of h, following an assumed instantaneous perturbation N_d' at $t = 0$ to the steady-state cloud droplet concentration $N_d^{(e)}$ is

$$\frac{dh}{dt} = \frac{dz_i}{dt} - \frac{dz_{\rm cb}}{dt}. \tag{1}$$

Next, we consider the response of the cloud base and cloud top separately.

a. Cloud-base response

We introduce the following two moist conserved variables: q_T, the total water mixing ratio (vapor + liquid), and $S_l = c_pT + gz - L_v q_l$, the liquid static energy. Here c_p is the specific heat of air at constant pressure, T is the temperature, z is the altitude, g is the gravitational acceleration, L_v is the latent heat of evaporation of water, and q_l is the liquid water content. The response of $z_{\rm cb}$ can be expressed as

$$\frac{dz_{\rm cb}}{dt} = \left(\frac{\partial z_{\rm cb}}{\partial q_T}\frac{\partial q_T}{\partial t} + \frac{\partial z_{\rm cb}}{\partial S_l}\frac{\partial S_l}{\partial t}\right). \tag{2}$$

The variables q_T and S_l are well mixed throughout the depth of the MBL and are conserved under phase changes (Bretherton and Wyant 1997), but can be modified by diabatic processes (such as precipitation and radiation), entrainment mixing, and surface fluxes. Budget equations for q_T and S_l can be written (e.g., Caldwell et al. 2005). To examine the rate of change of q_T and S_l in (2) resulting from the competing effects of changes in surface precipitation and entrainment, we assume that the effect upon the q_T and S_l budgets of changes in the net radiative flux divergence and the surface sensible and latent heat fluxes are small compared with changes in the surface precipitation and entrainment. In response to N_d', instantaneous perturbations $P_{\rm cb}'$, P_0', and w_e', the cloud-base and surface precipitation rates and the entrainment rate, respectively, are assumed. This is reasonable because the time scales for precipitation formation and turbulent kinetic energy adjustment that determine the response time of $P_{\rm cb}$, P_0, and w_e are of the order of an hour or less.

We can then write

$$M\frac{\partial q_T}{\partial t} = -P_0' + \rho_i w_e' \Delta q_T, \tag{3}$$

$$M\frac{\partial S_l}{\partial t} = L_v P_0' + \rho_i w_e' \Delta S_l, \tag{4}$$

where M is the mass of the MBL per unit area, ρ_i is the density at the inversion base, and Δx is the difference in x between the overlying air and the MBL.

It can be shown that $\partial z_{\rm cb}/\partial q_T = -(R_a T_{\rm cb}/g q_T)[(L_v R_a/c_p R_v T_{\rm cb}) - 1]^{-1}$ (see the appendix), where R_a and R_v are the gas constants for dry air and water vapor, and $T_{\rm cb}$ is the temperature of the cloud base. Similarly, $\partial z_{\rm cb}/\partial S_l = 1/g$ (see the appendix). These relations are com-

bined with (2), (3), and (4). Noting that $gM \approx p_0 z_i^{(e)}/H$, where $H = R_a T/g$ is the atmospheric scale height and p_0 is the surface pressure, we get an expression for dz_{cb}/dt as a function P_0' and w_e', namely,

$$\frac{dz_{cb}}{dt} = \frac{H}{p_0 z_i^{(e)}}[L_v P_0'(1 + \eta) + \rho_i w_e'(\Delta S_l - \eta L_v \Delta q_T)], \tag{5}$$

where $\eta = (R_a T_{cb}/L_v q_T)[(L_v R_d/c_p R_v T_{cb}) - 1]^{-1} \approx 0.8$ is roughly constant in the subtropical MBL. We relate P_0' and w_e' to N_d' assuming that the fractional perturbation in P_0 is equal to that in P_{cb}, so that

$$\frac{P_0'}{P_0^{(e)}} = \frac{P_{cb}'}{P_{cb}^{(e)}}. \tag{6}$$

To relate w_e' to P_{cb}' we consider the effect of precipitation on the convective velocity scale $w_* \equiv (2.5 \int_0^{z_i} \overline{w'b'}(z)\, dz)^{1/3}$, where $\overline{w'b'}(z)$ is the buoyancy flux, and upon the entrainment closure that relates w_e to w_*. The methodology for this, with S_l as the energy variable, is given in Caldwell et al. (2005), who present expressions relating $\overline{w'b'}(z)$ to the vertical fluxes of q_T and S_l required to maintain a mixed layer (see also Schubert et al. 1979; Bretherton and Wyant 1997). Making the simplifying assumptions that w_* is determined by the net radiative flux divergence across the MBL ΔR (Nicholls 1984) and that the change in P_0 has a negligible effect upon w_* compared with the change in P_{cb}, an approximate expression for w_e' can be derived (see the appendix) as

$$\frac{w_e'}{w_e^{(e)}} \approx -f(z_{cb}^{(e)}/z_i^{(e)}) \frac{L_v P_{cb}'}{\Delta R}, \tag{7}$$

where ΔR is positive for net radiation loss, and $f(\zeta = z_{cb}^{(e)}/z_i^{(e)}) = (\kappa\zeta + \epsilon)/[\beta + (1 - \beta)\zeta^2]$, with the thermodynamic coefficients $\beta \approx 0.6$ (Randall 1980), $\epsilon = c_p T/L_v \approx 0.11$, and $\kappa = 1 - \epsilon(1 + \delta) \approx 0.82$, because $\delta = 0.608$. Equation (7) expresses the leverage of precipitation upon the entrainment rate associated with its latent warming above z_{cb} and evaporative cooling below. For a given perturbation P_{cb}' and ΔR, the function $f(\zeta)$ results in $w_e'/w_e^{(e)}$, increasing with $z_{cb}^{(e)}/z_i^{(e)}$. This is because evaporative cooling of precipitation below z_{cb} exerts a stronger effect upon w_* than does the corresponding latent warming in the cloud layer.

Substitution of (6) and (7) into (5) leads to

$$\frac{dz_{cb}}{dt} = \frac{H}{p_0 z_i^{(e)}} L_v P_{cb}' \left[(1 + \eta) \frac{P_0^{(e)}}{P_{cb}^{(e)}} - f(z_{cb}^{(e)}/z_i^{(e)}) \frac{\rho_i w_e^{(e)}(\Delta S_l - \eta L_v \Delta q_T)}{\Delta R} \right], \tag{8}$$

the two terms of which, for $P_{cb}' < 0$, represent moistening/cooling resulting from suppression of precipitation and entrainment drying/warming caused by enhanced turbulence. Because we are concerned with microphysically driven precipitation perturbations, we relate P_{cb}' to the droplet concentration perturbation N_d' using a drizzle closure. Observational data (Pawlowska and Brenguier 2003; Comstock et al. 2004; Van Zanten et al. 2005) lend weight to closures of the form $P_{cb}'/P_{cb}^{(e)} = -K_D(N_d'/N_d^{(e)})$, where K_D is a positive constant. Substitution into (9) gives an expression for how z_{cb} responds to a perturbation in N_d,

$$\frac{dz_{cb}}{dt} = \frac{H}{p_0 z_i^{(e)}} K_D L_v P_{cb}^{(e)} \frac{N_d'}{N_d^{(e)}} \left[-(1 + \eta) \frac{P_0^{(e)}}{P_{cb}^{(e)}} + f(z_{cb}^{(e)}/z_i^{(e)}) \frac{\rho_i w_e^{(e)}(\Delta S_l - \eta L_v \Delta q_T)}{\Delta R} \right]. \tag{9}$$

b. Cloud-top response

Noting that $dz_i/dt = w_e'$, and expressing w_e' in terms of N_d' and the equilibrium state parameters as above, we arrive at an expression for dz_i/dt,

$$\frac{dz_i}{dt} = K_D L_v P_{cb}^{(e)} \frac{N_d'}{N_d^{(e)}} f(z_{cb}^{(e)}/z_i^{(e)}) \frac{w_e^{(e)}}{\Delta R}. \tag{10}$$

Thus, increasing cloud droplet concentration always leads to deepening of the MBL.

c. Cloud thickness response

Combining (9) and (10), we arrive at an expression for dh/dt of

$$\frac{dh}{dt} = \frac{HK_D L_v}{p_0 z_i^{(e)}} P_{cb}^{(e)} \frac{N_d'}{N_d^{(e)}} \left[(1 + \eta) \frac{P_0^{(e)}}{P_{cb}^{(e)}} + f(z_{cb}^{(e)}/z_i^{(e)}) \frac{w_e^{(e)}}{\Delta R} \chi \right], \tag{11}$$

where $\chi = p_0 z_i^{(e)}/H - (1 + \eta)(\Delta S_l - \eta L_v \Delta q_T)$. It can be seen from (11) that the second term, which represents the effect of entrainment on h, can be both positive or negative depending upon the sign of χ, a behavior previously explored by Randall et al. (1984).

To cast light on the influence of the environment on χ, we can approximately rewrite $\Delta S_l - \eta L_v \Delta q_T$ in terms of the free-tropospheric relative humidity RH_{FT}, such that $\Delta S_l - \eta L_v \Delta q_T \approx \alpha(1 - RH_{FT})$, where α weakly depends upon temperature and pressure and upon ΔS_l. In this way the sign of χ can be seen to be primarily determined by the MBL depth and the dryness of the free troposphere, and Fig. 1 shows a contour plot of $\chi \approx p_0 z_i^{(e)}/H - (1 + \eta)\alpha(1 - RH_{FT})$ against z_i and RH_{FT}

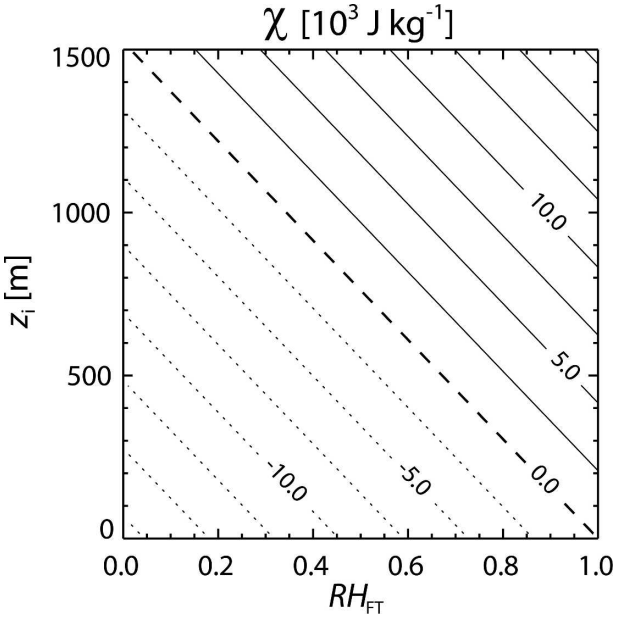

FIG. 1. Contour plot showing χ as a function of free-tropospheric relativity $\mathrm{RH_{FT}}$ and MBL depth z_i.

assuming a reference $T = 290$ K, $q_T = 8$ g kg^{-1}, $p_0 = 1020$ hPa, and $\Delta S_l = 8000$ J kg^{-1}. Changing ΔS_l within a reasonable range for the stratocumulus-topped MBL does not markedly change the results. Within the mixed layer framework, for MBLs with $\chi > 0$, an increase in N_d will *always* lead to a short time-scale response in which the cloud deepens, with a cloud thickness feedback that enhances the Twomey effect. However, the free troposphere over the eastern subtropical oceans is very dry, with $\mathrm{RH_{FT}}$ typically in the range of 10%–20% (Pierrehumbert 1995). Thus, even the deepest MBLs that can be treated as mixed layers (~1100 m) would have $\chi < 0$, so that entrainment perturbations alone lead to cloud thinning. However, we must also consider the moistening/cooling resulting from suppression of surface precipitation, that is, the first term in (11), to determine the sign of dh/dt. An important result here is that the *sign* of dh/dt is dependent upon the *fraction* of the precipitation that evaporates in the subcloud layer (i.e., $P_0^{(e)}/P_{cb}^{(e)}$), not upon its absolute magnitude.

Equation (11) can be used to understand the factors controlling the sign and magnitude of the cloud thickness response to perturbations in cloud droplet concentration at short time scales. First, we need to demonstrate the utility of the analytical form (11).

3. MLM formulation

To help determine the utility of (11) as a predictor of cloud thickness response at short time scales, we use a MLM that includes the key forcings impacting the MBL. The model is similar to that used in (Bretherton and Wyant 1997), but with a simplified vertical discretization that assumes piecewise linear behavior of the buoyancy flux in the cloud and subcloud layers, with sharp jumps at cloud top and base. Comparisons with a highly vertically discretized MLM show that the simplified treatment faithfully captures the general behavior of the mixed layer under different forcing conditions. The simplified form is faster and more analytically tractable than the discretized version.

The model has a simplified treatment of longwave radiation that allows flux divergence only at the cloud top and base. This assumption has been shown to induce only small errors (Schubert et al. 1979). The downward longwave flux at cloud top and the upward flux at cloud base are determined using the simple graybody scheme of (Welch and Zdunkowski 1976). Shortwave flux divergence is imposed only at the top of the cloud and increases in a physical manner with the liquid water path (LWP), with an analytical form derived using a fit to results from the radiative transfer model of Fu and Liou (1992). The results presented here are found to be insensitive to the details of the radiation treatment.

Surface sensible and latent heat fluxes are determined using bulk formulas as in Bretherton and Wyant (1997), with a surface wind speed of 7 m s^{-1}. The results are not strongly sensitive to this choice. Entrainment is parameterized using the Nicholls and Turton (1986) closure, with the evaporative enhancement constant set to 15 rather than 60, which compares more favorably with observations (Caldwell et al. 2005). Because entrainment is a key process in the response of h to changes in N_d, we examine the sensitivity of the results to changes in the entrainment closure in section 4d.

Precipitation at cloud base is parameterized using the formulation of Comstock et al. (2004)

$$P_{cb} = K_C(\mathrm{LWP}/N_d)^{1.75}, \tag{12}$$

with $K_C = 2.44 \times 10^{10}$ kg$^{-0.75}$ m$^{-3.75}$ s^{-1}. Thus, $K_D = 1.75$ for this closure [see previous section and Eq. (9)]. Other recent closures (Pawlowska and Brenguier 2003; Van Zanten et al. 2005) suggest values of K_D closer to unity, but this does not change the salient findings. In addition, the different sensitivity of precipitation to LWP may impact the equilibrium MBL state, and therefore (11); we explore this sensitivity in section 4d.

As we shall demonstrate, evaporation in the subcloud layer is extremely important and we use the formulation of Comstock et al. (2004) to estimate the surface precipitation P_0,

$$\frac{P_0}{P_{cb}} = \exp[-(z_{cb}/z_{evap})^{1.5}], \quad (13)$$

where z_{evap} is an evaporation-scale height that depends upon the mean radius of the drizzle drops, here assumed to be a constant 55 μm, leading to $z_{evap} = 475$ m. This constancy is supported by observations of Comstock et al. (2004) that show little correlation between P_{cb} and the mean drizzle drop radius. The formulation used compares favorably with aircraft data (Wood 2005a).

4. MLM simulations

To cover the range of external environmental conditions typically encountered over the subtropical eastern oceans, we conduct an ensemble of MLM simulations each with a different permutation of the three key forcing variables that control the equilibrium structure of the MBL. These are the (a) lower-tropospheric divergence D_0, (b) SST, and (c) free-tropospheric water vapor mixing ratio q_{FT}. Divergence D_0 determines the vertical profile of the subsidence rate $w_s(z) = D_0 z$. The 700-hPa potential temperature is set to 312 K, and so the effect of varying the SST primarily controls the lower-tropospheric stability (Klein and Hartmann 1993). The free-tropospheric moisture impacts the ability of entrainment to dry and warm the MBL. Table 1 lists the values of D_0, SST, and q_{FT} used. Three values of each give a total of 27 simulations.

The downwelling shortwave radiation at the top of the MBL is set to 140 W m^{-2}, close to the annual diurnal mean value over the subtropical belt. The diurnal cycle is not explicitly simulated. Despite there being a strong diurnal cycle of shortwave radiation, recent results from the southeast Pacific (Caldwell et al. 2005) suggest that the mixed layer concept is a reasonable approach to understanding the mean MBL structure over multiple diurnal cycles. We note that although the omission of the diurnal cycle in this study may limit the generalization of the findings, it does not invalidate the key findings. Further, Zhang et al. (2005) concluded that while the diurnal cycle of cloud thickness is strongly sensitive to the entrainment parameterization, the susceptibility of the mean state to changes in N_d does not depend strongly upon the representation of entrainment in large-scale models. We return to this in section 4d.

The strategy is to first run the MLM until it reaches equilibrium after several days for each of the 27 simulations in the ensemble. A time step of 1000 s is used throughout. These control simulations are all run to equilibrium with a control droplet concentration $N_d^e = 100$ cm^{-3}. When equilibrium has been reached, we then introduce a perturbation N_d' in the cloud droplet concentration. Initially, we assume that $N_d'/N_d^{(e)} = 0.05$, that is, the perturbation in N_d is 5% of the control. The extent to which the results depend upon the magnitude of the assumed $N_d^{(e)}$ and N_d' is examined in section 4d by varying these parameters. Throughout this study, we only include those cases where the buoyancy integral ratio, as defined in Turton and Nicholls (1987), is less than 0.2 at all times. This removes cases that are not well described using mixed layer theory. Our approach is essentially Lagrangian, but one for which the forcing conditions along the trajectory are held constant. We therefore require no advective treatment. In future work we plan to conduct simulations with evolving forcing conditions more typical of the subtropical eastern oceans, but this is beyond the scope of this work.

TABLE 1. Details of the external environmental conditions used

Parameter	Units	Values
D_0	10^{-6} s^{-1}	2, 3, 4
SST	K	288, 291, 294
q_{FT}	g kg^{-1}	1, 3, 6
θ_{700}	K	312

a. Indirect effect metric

As discussed above, increasing N_d leads to near-instantaneous increases in droplet surface area and therefore optical depth (the Twomey effect), and on longer time scales to feedbacks that can lead to changes in liquid water path and therefore cloud optical depth τ (the Albrecht effect). We write an expression (Pincus and Baker 1994) for the fractional response of τ to fractional changes in N_d as

$$\frac{d\ln\tau}{d\ln N_d} = \left(\frac{\partial\ln\tau}{\partial\ln N_d}\right)_h + \left(\frac{\partial\ln\tau}{\partial\ln h}\right)_{N_d}\left(\frac{\partial\ln h}{\partial\ln N_d}\right)_{ext}. \quad (14)$$

The first term on the rhs represents the Twomey effect (i.e., change in τ for fixed h) and the second the feedback related to changes in h subject to fixed external forcing conditions. For adiabatic clouds, which the clouds in the MLM are defined to be, $\tau \propto N_d^{1/3}h^{5/3}$ (Brenguier et al. 2000), so that (14) becomes

$$\frac{d\ln\tau}{d\ln N_d} = \frac{1}{3} + \frac{5}{3}\left(\frac{\partial\ln h}{\partial\ln N_d}\right)_{ext}. \quad (15)$$

From (15) we can define a ratio $\mathcal{R}_{IE}$ as the ratio of the second to first indirect effects, that is,

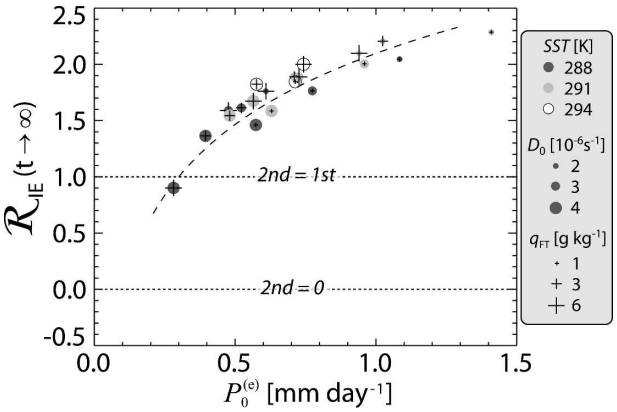

FIG. 2. Long time-scale indirect effect ratio $\mathcal{R}_{IE}$ as a function of the surface precipitation rate in the control run $P_0^{(e)}$ for the 27 runs. The symbol colors indicate SST, circle sizes represent D_0, cross sizes represent q_{FT}. The dashed curve represents an arbitrary fit to the data.

$$\mathcal{R}_{IE} = 5\left(\frac{\partial \ln h}{\partial \ln N_d}\right)_{ext}. \quad (16)$$

For example, for $\mathcal{R}_{IE} = 1$ the cloud thickness feedback acts to double the effect on τ of the instantaneous (Twomey) response. For $\mathcal{R}_{IE} = 0$ there is no feedback, and for $\mathcal{R}_{IE} = -1$ the feedback cancels the Twomey response. Thus, $\mathcal{R}_{IE}$ is a useful metric to evaluate cloud feedbacks associated with instantaneous increases in N_d. The time response of the cloud can be examined, at any arbitrary time t after the perturbation has been introduced, by deriving $\mathcal{R}_{IE}(t)$ by taking the derivative of $h(t)$ with respect to N_d in (16), that is,

$$\mathcal{R}_{IE}(t) = 5\{\ln[h(t)/h^{(e)}] - \ln[1 + N_d'/N_d^{(e)}]\}.$$

b. Equilibrium response

The long time-scale (equilibrium) response $\mathcal{R}_{IE}(t \to \infty)$ scales very well with the surface precipitation $P_0^{(e)}$ in the equilibrium state (Fig. 2). The value $\mathcal{R}_{IE}$ ranges from 0.9 to 2.4 with a median value of 1.8, indicating that the equilibrium response leads to a cloud thickness feedback that strongly enhances the Twomey effect. However, the time scale required to reach equilibrium has a median value of 4 days (not shown). This is comparable to the time that a typical air mass takes to advect across the subtropical stratocumulus regime and is longer than the typical time scales for aerosol depletion (discussed further below). It is therefore pertinent to examine the mixed layer response to changes at shorter time scales.

c. Short time-scale response

The mean value of $\mathcal{R}_{IE}$ averaged from $t = 0$ to $t = t_{max}$, where $t_{max} = 12$, 24, and 48 h (Fig. 3), indicate that

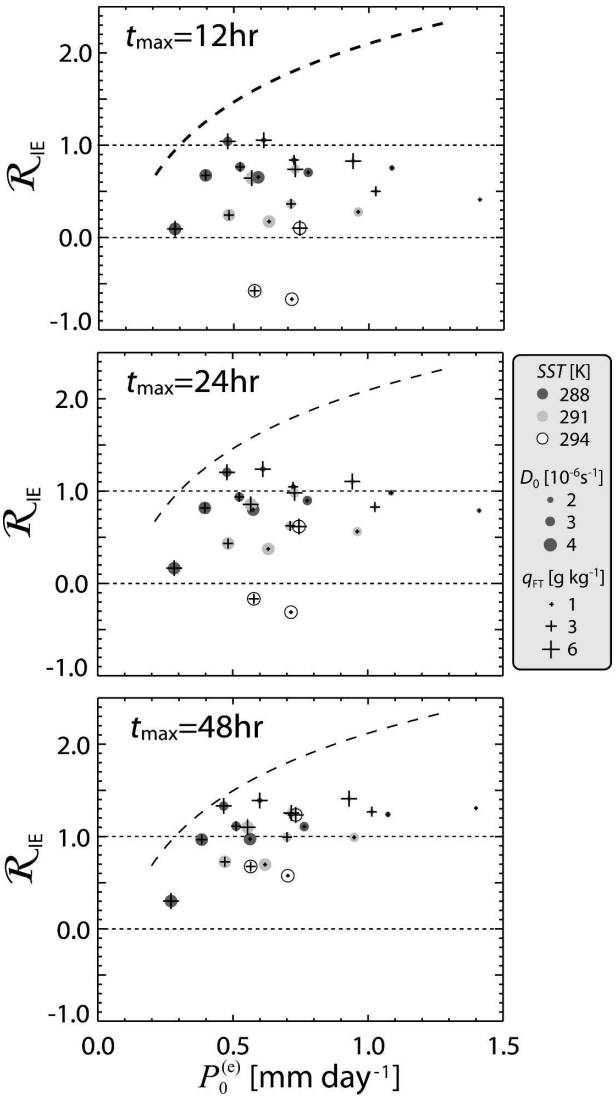

FIG. 3. Mean indirect effect ratio $\mathcal{R}_{IE}$ averaged from $t = 0$ to $t = t_{max}$ as a function of the surface precipitation rate in the control run $P_0^{(e)}$ for the 27 runs. Symbols are as Fig. 2. The dashed curve represents the fit to the equilibrium responses in Fig. 2.

when t_{max} is shorter than the equilibrium time scale, $\mathcal{R}_{IE}$ is smaller than $\mathcal{R}_{IE}(t \to \infty)$, and the scaling with $P_0^{(e)}$ is lost. Further, for $t_{max} < 24$ h, $\mathcal{R}_{IE}$ is in some cases negative, indicating cloud thinning as a response to increasing N_d. From the response at $t_{max} = 12$ h, we can see that the environmental conditions favoring $\mathcal{R}_{IE} < 0$ are weak static stability (high SST), with a somewhat weaker dependence upon D_0 and q_{FT}. In some cases, for fixed SST and D_0, a drier free troposphere results in lower values of $\mathcal{R}_{IE}$, which agrees with the general conclusion of Ackerman (2004). However, there are cases (e.g., SST = 298 K, $D_0 = 3 \times 10^{-6}$ s^{-1}) where this does not hold.

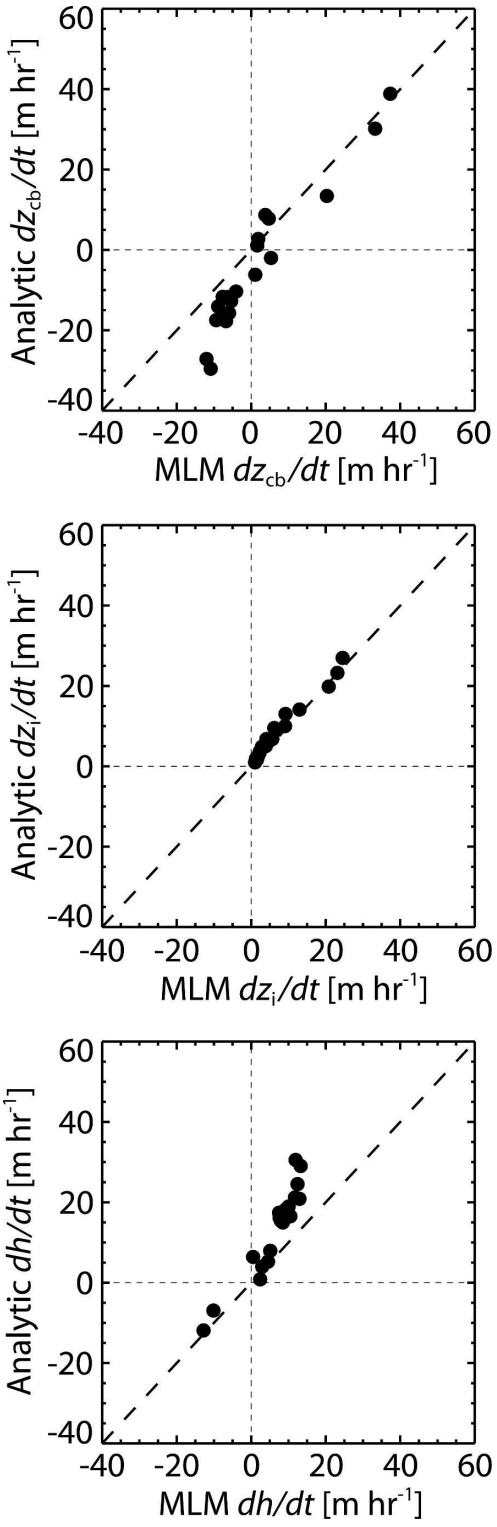

FIG. 4. Comparison of (a) dz_{cb}/dt, (b) dz_i/dt, and (c) dh/dt from the MLM simulations (abscissa) with the analytical forms given in (9), (10), and (11) for the range of environmental conditions described in Table 1. Values plotted are the rates normalized by the fractional N_d perturbation. The MLM tendencies were calculated over the period $0 < t < 8$ h. Only simulations for which the equilibrium control simulation has a buoyancy integral ratio (see Bretherton and Wyant 1997) less than 0.2 are plotted.

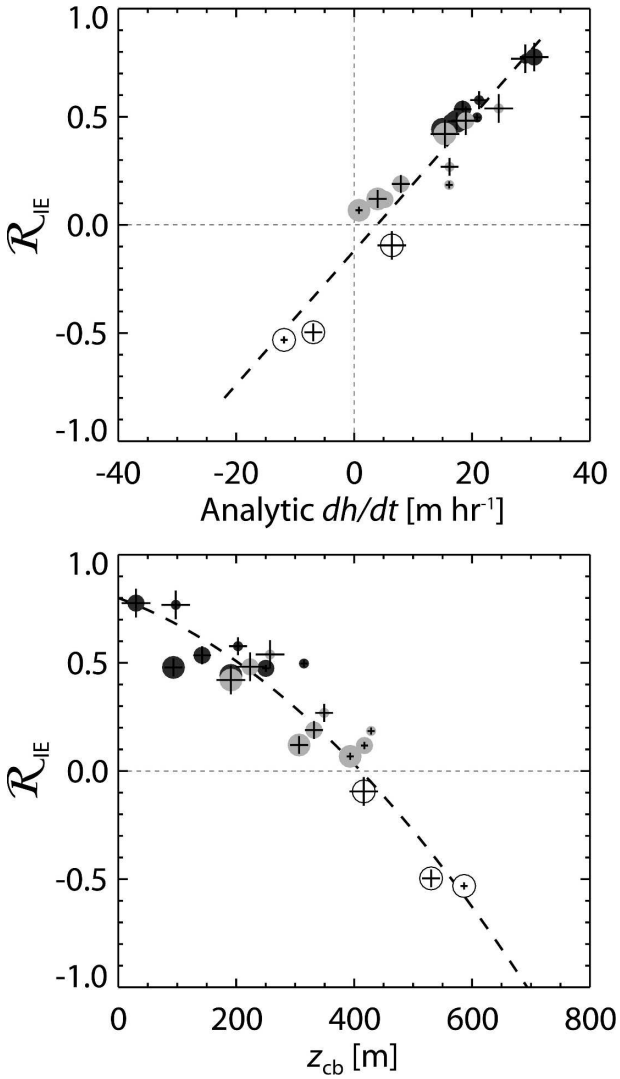

FIG. 5. The mean ratio, over $0 < t < 8$ h, of the Albrecht to Twomey effects $\mathcal{R}_{IE}$ as a function of (a) the analytic dh/dt formulation (11), and (b) the control cloud-base height $z_{cb}^{(e)}$. Symbols as in Fig. 2.

In section 2 approximate analytic expressions were derived for (9), (10), and thus (11) following the introduction of a perturbation in N_d. These expressions depend only upon the equilibrium state and the magnitude $N_d'/N_d^{(e)}$ of the perturbation. Figure 4 demonstrates, by comparison with the complete MLM, that the analytic tendencies for z_{cb}, z_i, and h, are reasonable approximations on short time scales. Figure 5 indicates that the analytical formulation (11) is a good predictor of $\mathcal{R}_{IE}$ (and hence the cloud thickness feedback) on short time scales. While the analytic form does not perform perfectly, as is most clearly seen in by the discrepancies in cloud-base height in Fig. 4a, the ability to analytically treat the general behavior of the MBL is

encouraging because it greatly simplifies the problem of understanding the physical controls upon the short time-scale response of the cloud thickness to changes in microphysics. Additional tests (not shown) demonstrate that feedbacks in h associated with changes in net radiative flux divergence and surface turbulent fluxes are of secondary importance in determining the response of the cloud thickness on time scales of 1 day or less. Nevertheless, these processes most likely do contribute to the discrepancies in Fig. 4.

Essentially then, the sign and magnitude of $\mathcal{R}_{\rm IE}$ is determined by the degree to which the entrainment cloud thinning/deepening is offset or enhanced by the precipitation suppression thickening. By examining (11), and the expression for χ, we can see that the key variables determining the sign of $\mathcal{R}_{\rm IE}$ are $P_0^{(e)}/P_{\rm cb}^{(e)}$, $f(z_{\rm cb}^{(e)}/z_i^{(e)})$, $w_e^{(e)}$, $z_i^{(e)}$, and $\mathrm{RH_{FT}}$.

The ratio of surface to cloud-base precipitation $P_0^{(e)}/P_{\rm cb}^{(e)}$, as described in (13), strongly decreases with $z_{\rm cb}$ because the greater falling distance and drier subcloud layer favors more precipitation evaporation. As described in section 2a $f(z_{\rm cb}^{(e)}/z_i^{(e)})$ increases with $z_{\rm cb}/z_i$. In a simplistic view of the equilibrium-state moisture budget of the MBL being roughly a balance between latent evaporation from the surface and entrainment drying, the product $w_e(1 - \mathrm{RH_{FT}})$ that appears in (11) will increase strongly with $z_{\rm cb}$. Thus, although (11) is a complex function of a number of parameters, many of them ultimately scale with $z_{\rm cb}$. Figure 5b indeed confirms that $\mathcal{R}_{\rm IE}$ is strongly tied to $z_{\rm cb}^{(e)}$ on short time scales. What is remarkable is that for $z_{\rm cb} > 400$ m, $\mathcal{R}_{\rm IE}$ becomes negative. Insofar as the MLM is a reasonable predictor of the behavior of the MBL as $z_{\rm cb}$ increases beyond 400 m (and this is questionable because the buoyancy integral ratio tends to exceed zero as $z_{\rm cb}$ increases), complete cancellation of the Twomey effect by cloud thinning (i.e., $\mathcal{R}_{\rm IE} = -1$) is expected when $z_{\rm cb} \approx 600$–700 m. Whether this is indeed a physically realistic MBL response will need to be examined using large-eddy simulation, which can simulate the MBL response during decoupling. Our results at least suggest the likely range of environmental conditions for which we might expect cancellation. As Fig. 5b shows, the $\mathcal{R}_{\rm IE} < 0$ response is predominantly determined by the lower-tropospheric stability (red circles), with an additional dependence upon $\mathrm{RH_{FT}}$. Lower stability favors deeper boundary layers (Wood and Hartmann 2006) and elevated cloud bases. A dry free troposphere not only leads to strong entrainment drying upon perturbing N_d as suggested by Ackerman (2004), but the drying also leads to equilibrium state that has an elevated cloud base and thus lower $P_0^{(e)}/P_{\rm CB}^{(e)}$.

d. Sensitivity to assumptions

It is important to ascertain the robustness of the findings in this study. Given that precipitation and entrainment are the key processes determining the response, we carry out sensitivity studies using the MLM to examine the influence of varying the parameterizations within reasonable bounds. In addition, we examine the sensitivity of the results to changes in the value of $N_d^{(e)}$ and N_d', that is, the base-state and perturbation droplet concentrations. Finally, we examine the possible consequences of considering advective terms in the MLM.

Doubling the precipitation efficiency factor K_C in (12) changes the relationship between $\mathcal{R}_{\rm IE}$ and $z_{\rm cb}^{(e)}$ (Fig. 6a), with stronger feedback (either positive or negative). A change in the evaporation-scale height $z_{\rm evap}$ resulting from a change in the drizzle drop mean radius from 49 to 65 μm has a very strong impact (Fig. 6). The results demonstrate the importance of accurately representing drizzle production, its size distribution, and its evaporation in the subcloud layer.

Changing the entrainment efficiency (Fig. 7a) also has little effect upon the form of the relationship between $\mathcal{R}_{\rm IE}$ and $z_{\rm cb}^{(e)}$, although it can be seen that, in general, the points have moved along the base-case curve because increased efficiency leads to deeper boundary layers with more elevated cloud bases and therefore a stronger drying effect upon perturbing N_d. A similar conclusion is reached (Fig. 7b) when we switch to an alternative entrainment closure (Lewellen and Lewellen 1998). The effect of different entrainment closures is primarily to influence the cloud-base height in the unperturbed state and thereby change the feedback sensitivity $\mathcal{R}_{\rm IE}$. Our conclusion therefore differs from that of Zhang et al. (2005) who suggest that aerosol indirect effects would not be strongly sensitive to the representation of entrainment. Here, we find a stronger second indirect effect (larger $\mathcal{R}_{\rm IE}$) for weaker entrainment efficiency because weaker entrainment leads to a lower cloud base and less evaporation of drizzle in the subcloud layer. The reasons for the different conclusions are unclear, but do not involve fundamental differences in the mechanics of the parameterizations used in the two studies and may stem from the fact that the Zhang et al. (2005) results represent equilibrium simulations, the behavior of which may be quite different to the short time-scale response.

The sensitivity to the assumed control concentration and the magnitude of the perturbation (Fig. 8) reveals that higher $N_d^{(e)}$ leads to weaker cloud thickness feedback (both positive and negative). This highlights that it is important to quantify the background or "preindustrial" cloud/aerosol microphysics to accurately deter-

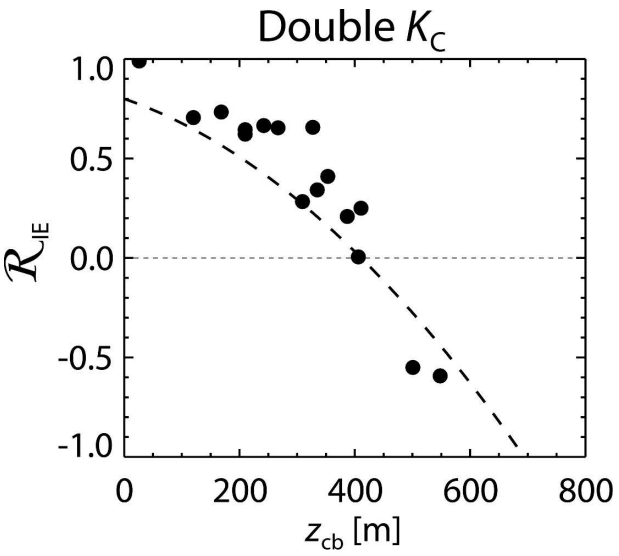

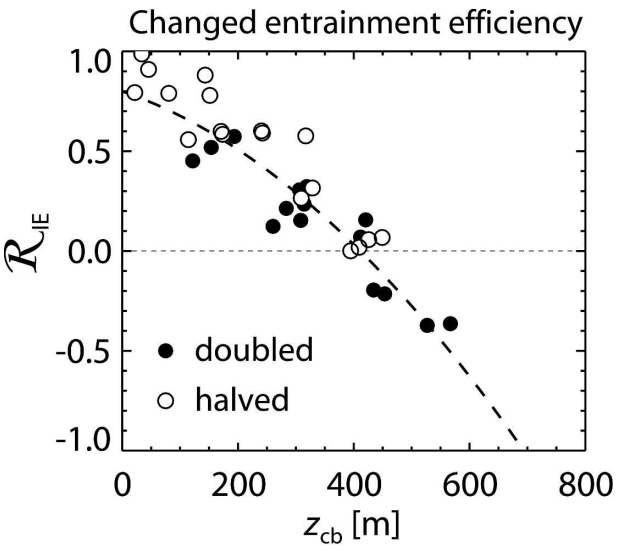

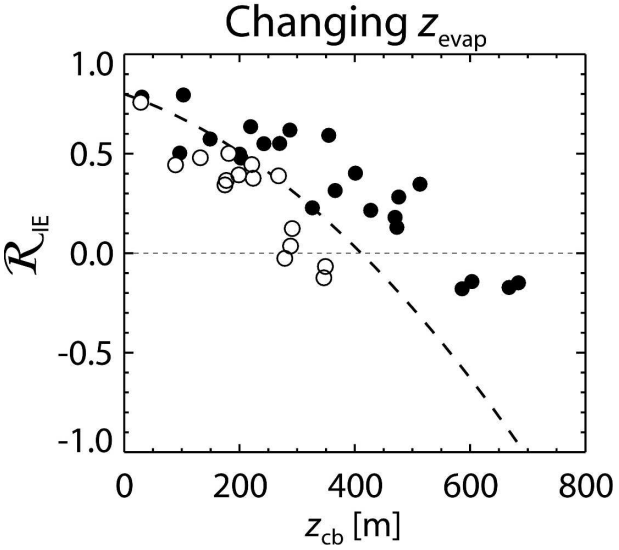

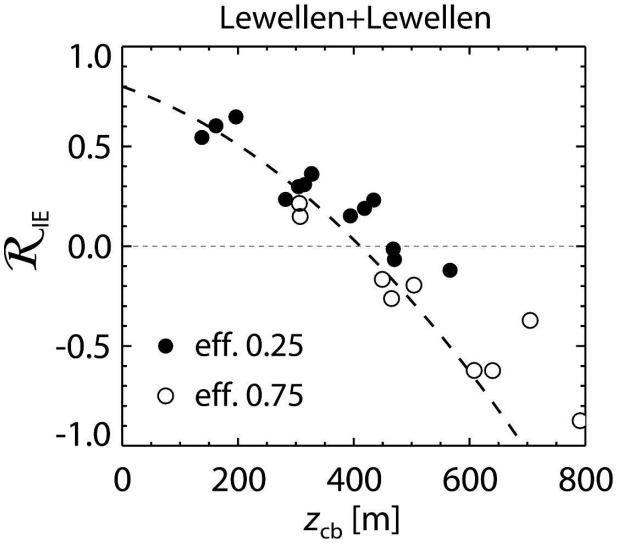

FIG. 6. Sensitivity of the relationship between $\mathcal{R}_{IE}$ and $z_{cb}^{(e)}$ to the representation of drizzle: (a) doubling the precipitation efficiency factor K_C in (12), and (b) varying the assumed mean radius of the drizzle drops from 49 (open circles) to 65 (solid circles) μm, which results in a 50% decrease and increase respectively in the evaporation-scale height z_{evap}. The dashed line represents the arbitrary fit to the data in the base case (Fig. 5).

FIG. 7. Same as Fig. 6, but for examining sensitivity to the representation of entrainment. Results show sensitivity to (a) doubling and halving the entrainment efficiency in the Turton–Nicholls parameterization, and (b) replacing the entrainment parameterization with an alternative closure of Lewellen and Lewellen (1998) with two values (0.25 and 0.75) of the entrainment efficiency. The dashed line represents the arbitrary fit to the data in the base case (Fig. 5).

mine the indirect effects. The results are quite insensitive to the magnitude of the perturbation, further demonstrating the robustness of the results, and lending support to the $\mathcal{R}_{IE}$ methodology that we have used in this study.

5. Discussion and conclusions

We have used a mixed layer framework to examine the key physical processes that determine the cloud thickness feedback response and to perturbations in cloud droplet concentration. Further, we have examined the sensitivity of the response to changes in the representation of these processes in the MLM. The advantage of the MLM is that it can be run very cheaply over a much wider range of external environmental conditions, allowing a more thorough exploration of the range of responses than can be achieved with more sophisticated models.

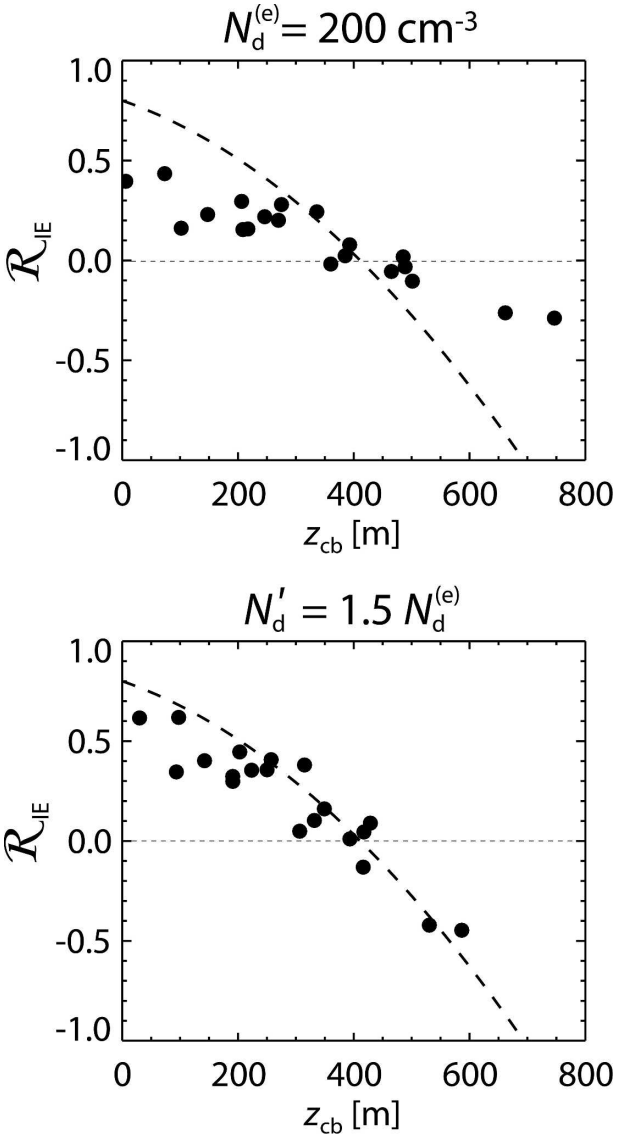

FIG. 8. Sensitivity of the relationship between $\mathcal{R}_{IE}$ and $z_{cb}^{(e)}$ to (a) doubling the control droplet concentration $N_d^{(e)}$ to 200 cm^{-3}, and (b) increasing the magnitude of the perturbation N_d' by a factor of 10. The dashed line represents the arbitrary fit to the data in the base case (Fig. 5).

At long time scales (greater than a few days), increases in cloud droplet concentration invariably result in thicker clouds and an Albrecht effect that is at least as strong as the Twomey effect, over a wide range of large-scale forcings. In this case, the ratio of the two effects, as expressed with the parameter $\mathcal{R}_{IE}$, increases with the surface precipitation rate in the unperturbed state.

The response over shorter time scales can be markedly different, and can be understood using an approximate analytic formulation. In this case, the cloud-top height does not have time to fully equilibrate, leading to much weaker, and in some cases even negative, cloud thickness changes when N_d is increased. Only when the cloud-base height is very low (<100 m) does the Albrecht effect rival the Twomey effect. The ratio $\mathcal{R}_{IE}$ decreases as the cloud-base height increases, and it is remarkable that much of the variance in $\mathcal{R}_{IE}$ across different cases can be explained by this parameter alone. This behavior can be rationalized physically. An elevated cloud base permits more precipitation evaporation before it reaches the surface. This has the following two effects: (i) greater evaporation limits the moistening/cooling of the MBL resulting from precipitation suppression, while allowing the suppressed precipitation to increase the entrainment drying/warming upon increasing N_d (as suggested by Ackerman 2004), and (ii) greater subcloud evaporation increases the leverage of any change in cloud-base precipitation on entrainment because evaporation in cloud-free subcloud air exerts a stronger effect upon w_* than in-cloud latent heating [see Eq. (7)]. In addition, a dry free troposphere is conducive to elevated cloud bases, and so not only does the dry free troposphere directly affect the degree to which entrained air will dry/warm the MBL, it also influences the unperturbed state so as to result in a strong dependence of $\mathcal{R}_{IE}$ on cloud-base height. On time scales of less than a day, feedbacks involving radiation and surface turbulent fluxes are relatively unimportant.

The importance of the time scale in determining the feedback response suggests that a theoretical understanding of aerosol cloud interactions will not be complete without being able to predict the time scale over which the CCN concentration is modified following the introduction of a perturbation. The two key modification processes in the subtropical MBL are likely to be (a) dilution of the MBL through entrainment of relatively clean free-tropospheric air, and (b) coalescence scavenging. The time scale of the former is $\tau_{dil} = D_0^{-1}$, that is, comparable to the time scale over which z_i is modified. This is relatively long (3–6 days). The time scale for coalescence scavenging τ_{scav} can be estimated using a theoretical treatment of the rate at which cloud droplets coalesce (Wood 2006), which gives

$$\tau_{scav} \approx \frac{16\rho_w z_i}{9E_0 h P_{cb}}, \tag{17}$$

where ρ_w is the density of liquid water and $E_0 \approx 4 \times 10^3$ m^{-1} is a constant related to the coalescence efficiency of small drops. The theory agrees well with detailed microphysical simulations (Feingold et al. 1996) and with rates derived by solving the stochastic collection

equation using observed cloud and drizzle size distributions (Wood 2005b). The inverse dependence of τ_{scav} on P_{cb} means that, for the MLM simulations plotted in Fig. 2, τ_{scav} ranges from 0.3 days for the cases with the highest $P_{cb}^{(e)}$ to roughly 1.5 days for the cases with the lowest $P_{cb}^{(e)}$. Given that there is a good correlation between $z_{cb}^{(e)}$ and $P_{cb}^{(e)}$($r = 0.85$), this implies that the short time-scale response is likely to be the most physically relevant in MBLs with higher z_{cb}. Essentially then, the value of $\mathcal{R}_{IE}$ integrated over the period $0 < t < \tau_{scav}$ may well be the most physically relevant assessment of the importance of the feedback effect in real MBLs. The results (not shown) look remarkably similar to Fig. 5b, but with somewhat more positive $\mathcal{R}_{IE}$ for $z_{cb}^{(e)} < 400$ m and slightly more negative $\mathcal{R}_{IE}$ at larger $z_{cb}^{(e)}$. However, preliminary steps at a prognostic treatment of CCN in the mixed layer framework reveal that the time scale for relaxation of an imposed perturbation depends in a subtle way upon the balance of sources and sinks that determine the background CCN concentration. This therefore suggests that the response to a CCN perturbation in the real MBL is not only dependent upon the magnitude of the perturbation and the state of the MBL at the time of the perturbation, but also upon the physical and chemical processes responsible for maintaining the CCN concentrations in the unperturbed state. In addition, the picture is further blurred because of the potential for drizzle feedback on the aerosol scavenging time scale. It is clear however that the time scale of the aerosol perturbation is important for understanding the magnitude (and even the sign) of the aerosol indirect effects.

We should emphasize that the mixed layer framework is somewhat limited in its scope, being useful as a tool for examining cloud and MBL behavior only when there are no substantial negative subcloud buoyancy fluxes. To alleviate the concerns over the MLM's validity somewhat, we restricted our analysis to cases where the buoyancy integral ratio, as defined in Turton and Nicholls (1987), is less than 0.2 at all times throughout both the control and the perturbation simulations, and so the MBL would be expected to remain well mixed in these cases. However, we suggest that more sophisticated models should be run to corroborate the findings presented here.

Finally, consequences of the findings are discussed. First, climate models used to simulate aerosol indirect effects have poor vertical resolution and tend to produce MBL clouds that are too close to the ocean surface (Bretherton et al. 2004). In the true subtropical MBL, observations suggest that although precipitation is very important, the amount of precipitation *reaching the surface* is quite low (Comstock et al. 2004; Van Zanten et al. 2005), and so the MBL moisture budget as a whole is largely determined by a balance between surface evaporation and entrainment drying. These are conditions that are favorable for small or even negative values of $\mathcal{R}_{IE}$. The poor representation of MBL clouds in climate models leads to an MBL moisture budget that is controlled more by a balance between surface evaporation and surface precipitation, with a weaker role for entrainment. Thus, the combined aerosol indirect effect feedbacks in these models may be artificially strong. It is suggested that single-column versions of the climate models could prove to be useful test beds to examine these feedbacks. Second, the results may also rationalize satellite observations of ship tracks (Coakley and Walsh 2002) that imply that liquid water path frequently *decreases* in ship tracks compared with the surrounding cloud.

Acknowledgments. The author thanks Peter Caldwell, Christopher Bretherton, Marcia Baker, and Bjorn Stevens for enlightening discussion of mixed layer theory.

APPENDIX

Derivation of Terms in Cloud-Base Height Response

In deriving (9), some assumptions were made to simplify the formulation. Here we present a more complete derivation of some of these terms.

a. *Response of cloud-base height to total water content*

First, we need an expression for $\partial z_{cb}/\partial q_T$,

$$\frac{\partial z_{cb}}{\partial q_T} = \frac{\partial z_{cb}}{\partial q_s(z_{cb})}, \tag{A1}$$

where $q_s(z_{cb})$ is the saturation mixing ratio at the cloud base z_{cb}. Writing $q_s(z_{cb})$ as a function of the cloud-base temperature T_{cb} and pressure p_{cb}, we can write

$$\frac{\partial q_s(z_{cb})}{\partial z_{cb}} = \frac{\partial q_s(z_{cb})}{\partial T_{cb}}\frac{\partial T_{cb}}{\partial z_{cb}} + \frac{\partial q_s(z_{cb})}{\partial p_{cb}}\frac{\partial p_{cb}}{\partial z_{cb}}. \tag{A2}$$

Now we apply the Clausius–Clapeyron equation, noting that $\partial T_{cb}/\partial z_{cb} = g/c_p$, $\partial p_{cb}/\partial z_{cb} \approx p/H$ (where $H = R_a T/c_p$ is the scale height), and $\partial q_s(z_{cb})/\partial p_{cb} = q_T/p_{cb}$, and we obtain

$$\frac{\partial q_s(z_{cb})}{\partial z_{cb}} = -\frac{g q_T}{R_a T_{cb}}\left(\frac{L_v R_a}{c_p R_v T_{cb}} - 1\right), \tag{A3}$$

where g is the gravitational acceleration, L_v is the latent heat of evaporation of water, R_a and R_v are the gas

constants for dry air and water vapor, respectively, and c_p is the specific heat of air at constant pressure. Thus,

$$\frac{\partial z_{cb}}{\partial q_T} = -\frac{R_a T_{cb}}{g q_T}\left(\frac{L_v R_a}{c_p R_v T_{cb}} - 1\right)^{-1}. \quad \text{(A4)}$$

b. Response of cloud-base height to liquid static energy

The expression for $\partial z_{cb}/\partial S_l$ can be derived using

$$\frac{\partial z_{cb}}{\partial S_l} = \frac{\partial z_{cb}}{\partial T_{cb}}\frac{\partial T_{cb}}{\partial S_l} = \frac{c_p}{g}\frac{1}{c_p} = 1/g. \quad \text{(A5)}$$

c. Entrainment response to precipitation perturbations

Equation (7) gives an approximate expression relating the perturbation P'_{cb} in cloud base precipitation rate to that in entrainment rate w'_e. This is derived as follows.

First, we assume that the buoyancy flux profile $\langle w'b'\rangle(z)$ in the MBL is piecewise linear and set by values at four defining levels: the surface, just below cloud base z_{cb}^-, just above cloud base z_{cb}^+, and just below the inversion z_i. Following Bretherton and Wyant (1997) we relate $\langle w'b'\rangle(z)$ to the vertical flux $\langle w'S'_v\rangle(z)$ of virtual static energy $S_v = c_p T_v + gz$, where T_v is the virtual temperature (including liquid loading), that is, $\langle w'b'\rangle(z) = (g/S_{v0})\langle w'S'_v\rangle(z)$, where S_{v0} is the reference (surface) virtual static energy.

Next, following Bretherton and Wyant (1997), we write expressions for the virtual static energy flux at the four defining levels, making the following assumptions: (a) latent and sensible heat fluxes do not contribute to the buoyancy flux; (b) entrainment does not contribute to the buoyancy flux; (c) radiative flux divergence ΔR occurs only at the cloud top (Schubert et al. 1979); and (d) precipitation rate is maximal at the cloud base P_{cb}, and decreases linearly to zero at the surface and the cloud top. We can then write

$$\langle w'S'_v\rangle(0) = 0, \quad \text{(A6)}$$

$$\langle w'S'_v\rangle(z_{cb}^-) = \zeta\Delta R/\rho - L_v P_{cb}/(1 - \epsilon\delta)/\rho, \quad \text{(A7)}$$

$$\langle w'S'_v\rangle(z_{cb}^+) = \beta\zeta\Delta R/\rho - \epsilon L_v P_{cb}/\rho, \quad \text{(A8)}$$

$$\langle w'S'_v\rangle(z_i) = \beta\Delta R/\rho, \quad \text{(A9)}$$

where $\zeta = z_{cb}/z_i$ is the normalized cloud-base height, ρ is a reference air density, and the thermodynamic coefficients are $\beta \approx 0.6$, $\delta = 0.608$, and $\epsilon = c_p T/L_v \approx 0.11$ (Randall 1980).

We then make the assumption that, given a perturbation P'_{cb} in the cloud-base precipitation rate, the fractional perturbation in entrainment rate $w'_e/w_e^{(e)}$ is simply equal to the fractional perturbation in the vertically integrated buoyancy flux $B'/B^{(e)}$, where $B^{(e)} = \int_0^{z_i}\langle w'b'\rangle\, dz$ for this minimalist flux profile can be simply calculated from (A6) to (A9). Some manipulation gives

$$B' = \frac{g}{2\rho S_{v0}} L_v P'_{cb}(\kappa\zeta + \epsilon), \quad \text{(A10)}$$

where $\kappa = 1 - \epsilon(1 + \delta) \approx 0.82$. A further approximation involves assuming that in the equilibrium state the precipitation has only a minor impact upon B, so that

$$B^{(e)} = \frac{g}{2\rho S_{v0}}\Delta R[\zeta^2(1 - \beta) + \beta]. \quad \text{(A11)}$$

Combining (A10) and (A11) leads to Eq. (7). Of course, it would be possible to derive a more complete expression in which the precipitation, entrainment, and surface fluxes are not assumed to play a negligible role in the buoyancy flux, but our simple formula captures the essence of the physical problem while remaining tractable.

REFERENCES

Ackerman, A. S., 2004: The impact of humidity above stratiform clouds on indirect aerosol climate forcing. *Nature,* **432,** 1014–1017.

Albrecht, B. A., 1989: Aerosols, cloud microphysics, and fractional cloudiness. *Science,* **245,** 1227–1230.

Anderson, T. L., R. J. Charlson, S. E. Charlson, R. Knutti, O. Boucher, H. Rodhe, and J. Heintzenberg, 2003: Climate forcing by aerosols—A hazy picture. *Science,* **300,** 1103–1104.

Bates, T. S., and Coauthors, 1998: Processes controlling the distribution of aerosol particles in the marine boundary layer during ACE 1. *J. Geophys. Res.,* **103,** 16 369–16 384.

Brenguier, J. L., and Coauthors, 2000: An overview of the ACE-2 CLOUDYCOLUMN closure experiment. *Tellus,* **52B,** 815–827.

Bretherton, C. S., and M. C. Wyant, 1997: Moisture transport, lower-tropospheric stability, and decoupling of cloud-topped boundary layers. *J. Atmos. Sci.,* **54,** 148–167.

——, T. Uttal, C. W. Fairall, S. E. Yuter, R. A. Weller, D. Baumgardner, K. Comstock, and R. Wood, 2004: The EPIC 2001 stratocumulus study. *Bull. Amer. Meteor. Soc.,* **85,** 967–977.

Caldwell, P., R. Wood, and C. S. Bretherton, 2005: Mixed-layer budget analysis of the diurnal cycle of entrainment in southeast Pacific stratocumulus. *J. Atmos. Sci.,* **62,** 3775–3791.

Coakley, J. A. J., and C. D. Walsh, 2002: Limits to the aerosol indirect radiative effect derived from observations of ship tracks. *J. Atmos. Sci.,* **59,** 668–680.

Comstock, K., R. Wood, S. Yuter, and C. S. Bretherton, 2004: Radar observations of precipitation in and below stratocumulus clouds. *Quart. J. Roy. Meteor. Soc.,* **130,** 2891–2918.

Feingold, G., S. M. Kreidenweis, B. Stevens, and W. R. Cotton, 1996: Numerical simulations of stratocumulus processing of cloud condensation nuclei through collision-coalescence. *J. Geophys. Res.,* **101,** 21 391–21 402.

Fu, Q., and K.-N. Liou, 1992: On the correlated k-distribution method for radiative transfer in nonhomogenous atmospheres. *J. Atmos. Sci.,* **49,** 2139–2156.

Ghan, S. J., and Coauthors, 2001: A physically-based estimate of

the radiative forcing by anthropogenic sulfate aerosols. *J. Geophys. Res.,* **106,** 5279–5293.

Haywood, J. M., and O. Boucher, 2000: Estimates of the direct and indirect radiative forcing due to tropospheric aerosols: A review. *Rev. Geophys.,* **38,** 513–543.

Jiang, H., G. Feingold, and W. R. Cotton, 2002: Simulations of aerosol-cloud-dynamical feedbacks resulting from entrainment of aerosol into the marine boundary layer during the Atlantic Stratocumulus Transition Experiment. *J. Geophys. Res.,* **107,** 4813, doi:10.1029/2001JD001502.

Katoshevski, D., A. Nenes, and J. H. Seinfeld, 1999: A study of processes that govern the maintenance of aerosols in the marine boundary layer. *J. Aerosol Sci.,* **30,** 503–532.

Klein, S. A., and D. L. Hartmann, 1993: The seasonal cycle of low stratiform clouds. *J. Climate,* **6,** 1588–1606.

Lewellen, D. C., and W. S. Lewellen, 1998: Large-eddy boundary layer entrainment. *J. Atmos. Sci.,* **55,** 2645–2665.

Lilly, D. K., 1968: Models of cloud-topped mixed layers under a strong inversion. *Quart. J. Roy. Meteor. Soc.,* **94,** 292–309.

Lohmann, U., and J. Feichter, 2005: Global indirect aerosol effects: A review. *Atmos. Chem. Phys.,* **5,** 715–737.

Ma, C. C., C. R. Mechoso, A. W. Robertson, and A. Arakawa, 1996: Peruvian stratus clouds and the tropical pacific circulation: A coupled ocean–atmosphere GEM study. *J. Climate,* **9,** 1635–1645.

Nicholls, S., 1984: The dynamics of stratocumulus: Aircraft observations and comparisons with a mixed layer model. *Quart. J. Roy. Meteor. Soc.,* **110,** 783–820.

——, and J. D. Turton, 1986: An observational study of the structure of stratiform cloud sheets: Part II. Entrainment. *Quart. J. Roy. Meteor. Soc.,* **112,** 461–480.

Pawlowska, H., and J. L. Brenguier, 2003: An observational study of drizzle formation in stratocumulus clouds for general circulation model (GCM) parameterizations. *J. Geophys. Res.,* **108,** 8630, doi:10.1029/2002JD002679.

Pierrehumbert, R. T., 1995: Thermostats, radiator fins, and the local runaway greenhouse. *J. Atmos. Sci.,* **52,** 1784–1806.

Pincus, R., and M. B. Baker, 1994: Effect of precipitation on the albedo susceptibility of clouds in the marine boundary layer. *Nature,* **372,** 250–252.

Randall, D. A., 1980: Conditional instability of the first kind upside down. *J. Atmos. Sci.,* **37,** 125–130.

——, J. A. Coakley, C. W. Fairall, R. A. Knopfli, and D. H. Lenschow, 1984: Outlook for research on marine subtropical stratocumulus clouds. *Bull. Amer. Meteor. Soc.,* **65,** 1290–1301.

Schubert, W. H., J. S. Wakefield, E. J. Steiner, and S. K. Cox, 1979: Marine stratocumulus convection. Part I: Governing equations and horizontally homogeneous solutions. *J. Atmos. Sci.,* **36,** 1286–1307.

Stevens, B., W. R. Cotton, G. Feingold, and C.-H. Moeng, 1998: Large-eddy simulations of strongly precipitating, shallow, stratocumulus-topped boundary layers. *J. Atmos. Sci.,* **55,** 3616–3638.

Turton, J. D., and S. Nicholls, 1987: A study of the diurnal variation of stratocumulus using a multiple mixed layer model. *Quart. J. Roy. Meteor. Soc.,* **113,** 969–1009.

Twomey, S., 1977: The influence of pollution on the shortwave albedo of clouds. *J. Atmos. Sci.,* **34,** 1149–1152.

Van Zanten, M. C., B. Stevens, G. Vali, and D. Lenschow, 2005: Observations of drizzle in nocturnal marine stratocumulus. *J. Atmos. Sci.,* **62,** 88–106.

Welch, R., and W. Zdunkowski, 1976: A radiation model of the polluted atmospheric boundary layer. *J. Atmos. Sci.,* **33,** 2170–2184.

Wood, R., 2005a: Drizzle in stratiform boundary layer clouds. Part I: Vertical and horizontal structure. *J. Atmos. Sci.,* **62,** 3011–3033.

——, 2005b: Drizzle in stratiform boundary layer clouds. Part II: microphysical aspects. *J. Atmos. Sci.,* **62,** 3034–3050.

——, 2006: The rate of loss of cloud droplets by coalescence in warm clouds. *J. Geophys. Res.,* **111,** D21205, doi:10.1029/2006JD007553.

——, and D. L. Hartmann, 2006: Spatial variability of liquid water path in marine boundary layer clouds: The importance of mesoscale cellular convection. *J. Climate,* **19,** 1748–1764.

Zhang, Y., B. Stevens, and M. Ghil, 2005: On the diurnal cycle and susceptibility to aerosol concentration in a stratocumulus-topped mixed layer. *Quart. J. Roy. Meteor. Soc.,* **131,** 1567–1583.

Response of cloud base height to changes in boundary layer moisture and heat content

We will formulate the tendency of cloud base height in terms of two moist conserved variables: q_T, the total water mixing ratio (which is the sum of the vapor mixing ratio and the liquid water mixing ratio $q_T = q_v + q_l$), and θ_l, the liquid potential temperature ($\theta_l = \theta - \frac{1}{\Pi}\frac{L_v}{c_p}\, q_l$). Cloud base height corresponds to the height at which the saturation mixing ratio (q_s) is equal to the total water mixing ratio:

$$q_s(T_{cb}, P_{cb}) = q_T \quad (1)$$

where T_{cb}, P_{cb} are the temperature and pressure values evaluated at the cloud base height.

Response of cloud base height to changes in moisture

Consider the case where there is a change in total water mixing ratio (dq_T) and liquid potential temperature is kept constant ($d\theta_l = 0$). From the definition of cloud base height we can write:

$$dq_T = dq_s(T_{cb}, P_{cb}). \quad (2)$$

We can define the total differential of the saturation mixing ratio as follows:

$$dq_s = \frac{\partial q_s}{\partial T}\, dT + \frac{\partial q_s}{\partial P}\, dP. \quad (3)$$

Thus we can formulate the response cloud base height (z_{cb}) to a change in the total water mixing ratio as follows:

$$\frac{dq_T}{dz_{cb}} = \frac{dq_s(T_{cb}, P_{cb})}{dz_{cb}} = \frac{\partial q_s}{\partial T}\frac{dT_{cb}}{dz_{cb}} + \frac{\partial q_s}{\partial P}\frac{dP_{cb}}{dz_{cb}}. \quad (4)$$

Taking the derivative the saturation mixing ratio with respect to temperature, we obtain $\frac{\partial q_s(z_b)}{\partial T_b} = \varepsilon \frac{\partial e_S}{\partial T_b}\frac{1}{P}\left(1 + \frac{e_s}{P}\right)$. Utilizing the Clausius Clapeyron equation $\left(\frac{\partial e_S}{\partial T_b} = \frac{L_v e_s}{R_v {T_b}^2}\right)$ and assuming that $\frac{e_s}{P} \ll 1$, we obtain:

$$\frac{\partial q_s(z_b)}{\partial T} = \frac{L_v q_T}{R_v {T_b}^2}. \quad (5)$$

Since there is no addition of heat to the boundary layer (Fig. 1) , we can utilize the dry adiabatic lapse rate to formulate $\frac{dT_{cb}}{dz_{cb}}$ as follows:

$$\frac{dT_{cb}}{dz_{cb}} = -\frac{g}{c_p} \quad (6)$$

Taking the partial derivative of the saturation mixing ratio ($q_s = \varepsilon \frac{e_S}{P - e_s}, \varepsilon = \frac{M_v}{M_d} = 0.622$) with respect to temperature and assuming that $p \gg e_S$, we obtain:

$$\frac{\partial q_s(z_b)}{\partial P} \approx -\frac{q_T}{P_{cb}}. \quad (7)$$

Applying the hydrostatic balance at the cloud base, we obtain:

$$\frac{dP_{cb}}{dz_{cb}} \approx -\frac{P_{cb} g}{R_d T_{cb}}. \quad (8)$$

Finally, substituting equations 5, 6, 7 and 8 into equation 4:

$$\frac{dz_{cb}}{dq_T} = \frac{R_d T_{cb}}{g q_T}\left(1 - \frac{L_v R_d}{c_p R_v T_{cb}}\right)^{-1} \quad (9)$$

a)

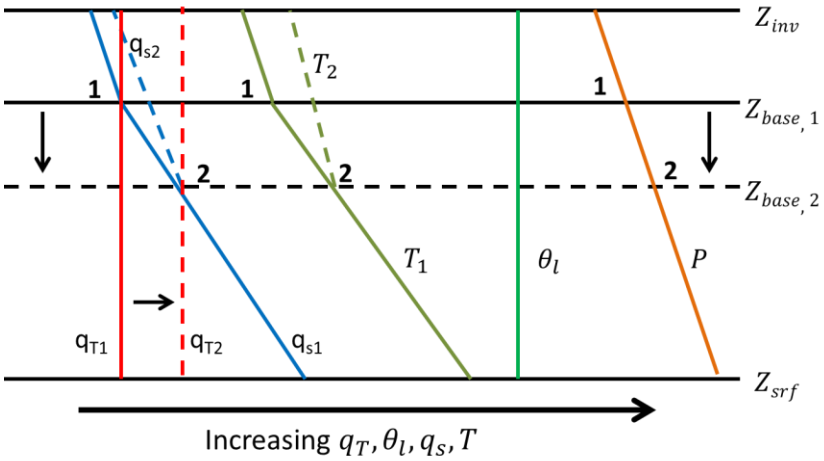

b)

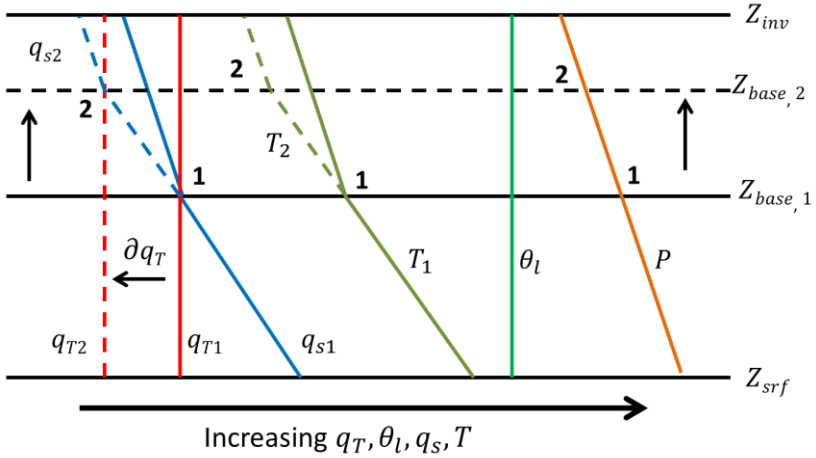

Figure 1a) response of cloud base height to an *increase* in total water mixing ratio, **b)** response of cloud base height to a *decrease* in total water mixing ratio

Response of cloud base height to changes in heat

Now, consider the case where there is a change in the liquid potential temperature ($d\theta_l$) and the total water mixing ratio is kept constant ($dq_T = 0$). Since $q_l = 0$ at the cloud base, we can express $d\theta_l$ at the cloud base as follows:

$$d\theta_l = \frac{dT_{cb}}{\Pi_1} - \frac{T_1}{\Pi_1^2} d\Pi_{cb} \quad (10)$$

where dT_{cb} is the difference in temperature at the different cloud bases. **It is important to note that $\boldsymbol{dT_{cb}}$ does not follow either the dry or moist adiabatic lapse rate as the vertical temperature profile is shifted due to the addition of heat in the boundary layer** (Fig. 2). $d\Pi_{cb}$ is the difference in exner function values at the different cloud base heights. Utilizing the definition of the exner function and assuming the atmosphere is in hydrostatic balance (equation 8), we can rewrite equation 10 in terms of dz_{cb}:

$$d\theta_l = \frac{dT_{cb}}{\Pi_1} - \frac{R_d T_1}{c_p \mathrm{P}_1 \Pi_1} dP_{cb} = \frac{1}{\Pi_1}\left(dT_{cb} + \frac{g}{c_p} d\mathrm{z}_{cb}\right)$$

$$\frac{d\theta_l}{d\mathrm{z}_{cb}} = \frac{1}{\Pi_1}\left(\frac{dT_{cb}}{d\mathrm{z}_{cb}} + \frac{g}{c_p}\right). \quad (11)$$

Since q_T is constant, q_s at the cloud base remains constant as well ($q_{s1} = q_{s2}$). Then we can equate the saturation mixing ratios at the cloud base as follows: $q_{s1} = \frac{e_{s1}}{P_1} = \frac{e_{s2}}{P_2}$; hence, $\frac{de_s}{e_{s1}} = \frac{dP}{P_1}$. Utilizing the definition of the saturation water vapor pressure($e_s = e_{s,tr} \exp\left[\frac{L_v}{R_v}\left(\frac{1}{T_{tr}} - \frac{1}{T}\right)\right]$ and the hydrostatic balance assumption, we can derive an expression for $\frac{dT_{cb}}{d\mathrm{z}_{cb}}$ as follows:

$$de_{s_{cb}} = e_{s,tr} \frac{L_v}{R_v T_1^2} \exp\left[\frac{L_v}{R_v}\left(\frac{1}{T_{tr}} - \frac{1}{T}\right)\right] dT_{cb} = \frac{L_v e_{s1}}{R_v T_{cb}^2} dT_{cb}$$

$$\frac{de_{s_{cb}}}{e_{s1}} = \frac{dP_{cb}}{P_1} = -\frac{g}{R_d T_{cb}} d\mathrm{z}_{cb}$$

$$\frac{de_{s_{cb}}}{e_{s1}} = \frac{L_v}{R_v T_1^2} dT_{cb} = -\frac{g}{R_d T_{cb}} d\mathrm{z}_{cb}$$

$$\frac{dT_{cb}}{d\mathrm{z}_{cb}} = -\frac{g R_v T_{cb}}{R_d L_v}. \quad (12)$$

Substituting equation 12 into 11:

$$\frac{d\theta_l}{d\mathrm{z}_{cb}} = \frac{g}{\mathrm{c_p} \Pi_1}\left(1 - \frac{c_p R_v T_{cb}}{R_d L_v}\right). \quad (13)$$

We can also derive an equation for the response of cloud base to changes in liquid static energy (s_l):

$$ds_l = c_p dT + g dz$$

$$\frac{ds_l}{dz_{cb}} = c_p \frac{dT}{dz_{cb}} + g$$
$$\frac{ds_l}{dz_{cb}} = g\left(1 - \frac{c_p R_v T_{cb}}{R_d L_v}\right) \quad (14)$$

Where we assumed that $dq_l = 0$ at the cloud base and substituted equation 12 for $\frac{dT_{cb}}{dz_{cb}}$.

a)

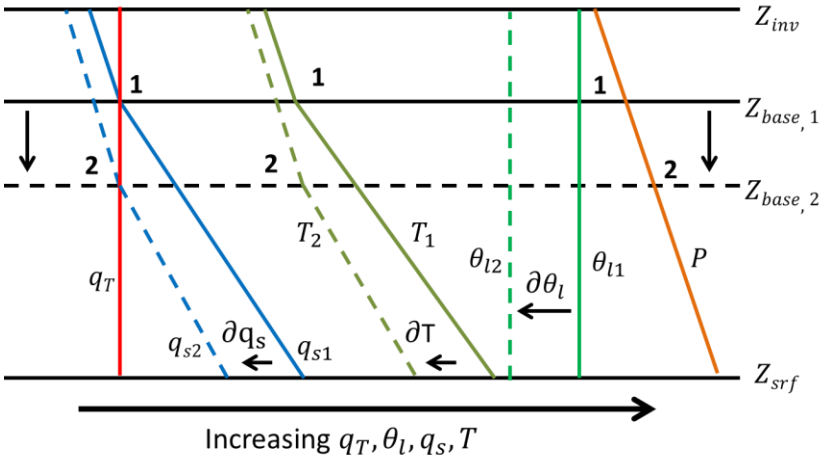

b)

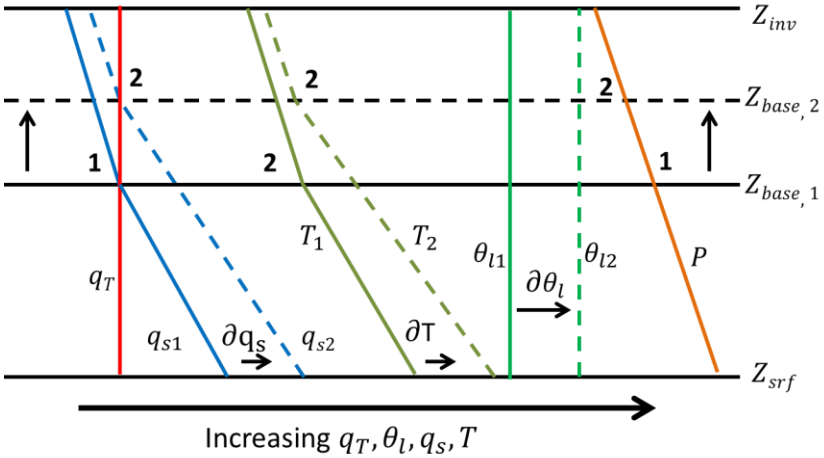

Figure 2 a) response of cloud base height to an *decrease* in liquid potential temperature, **b)** response of cloud base height to a in *increase* liquid potential temperature.